

## Supporting Information

### **Controllable synthesis and biomedical applications of bismuth-based nanospheres: enhanced photothermal therapy and CT imaging efficiency**

Dongxun Chen<sup>†a</sup>, Baowang Miao<sup>†b,c</sup>, Guidong Zhu<sup>b</sup>, Yanjie Liang<sup>\*a</sup> and Chengwei Wang<sup>\*b</sup>

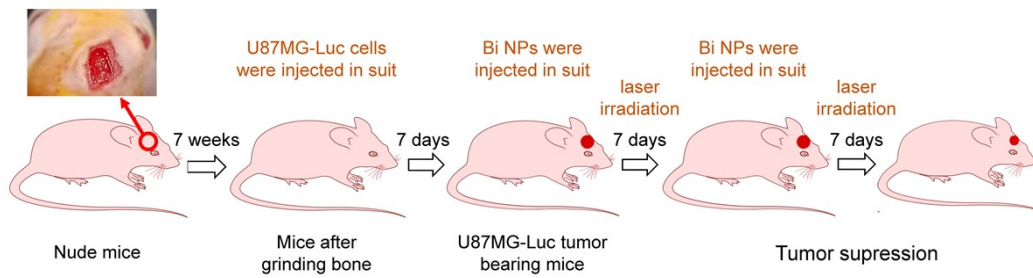
<sup>a</sup>Key Laboratory for Liquid-Solid Structure Evolution and Processing of Materials, Ministry of Education, Shandong University, Jinan 250061, China.

<sup>b</sup>Department of Neurosurgery, The Second Hospital of Shandong University, Jinan 250033, China.

<sup>c</sup>Department of Neurosurgery, Yiyuan County People's Hospital, Zibo 256100, China.

\*Corresponding authors: Yanjie Liang, Chengwei Wang

E-mail: [yanjie.liang@sdu.edu.cn](mailto:yanjie.liang@sdu.edu.cn); [wangchengwei@sdu.edu.cn](mailto:wangchengwei@sdu.edu.cn)



**Scheme S1.** Schematic diagram of photothermal therapy in tumor-bearing mice.

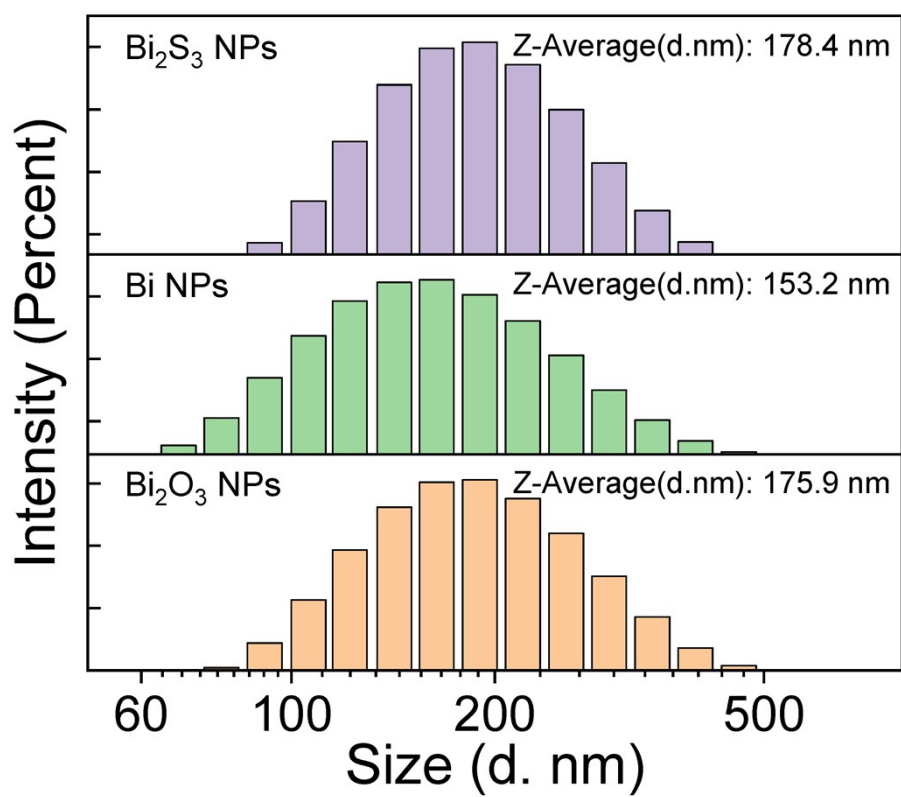


**Figure S1.** Typical DLS curve of the size distribution of the obtained Bi<sub>2</sub>S<sub>3</sub> NPs, Bi NPs, and Bi<sub>2</sub>O<sub>3</sub> NPs.

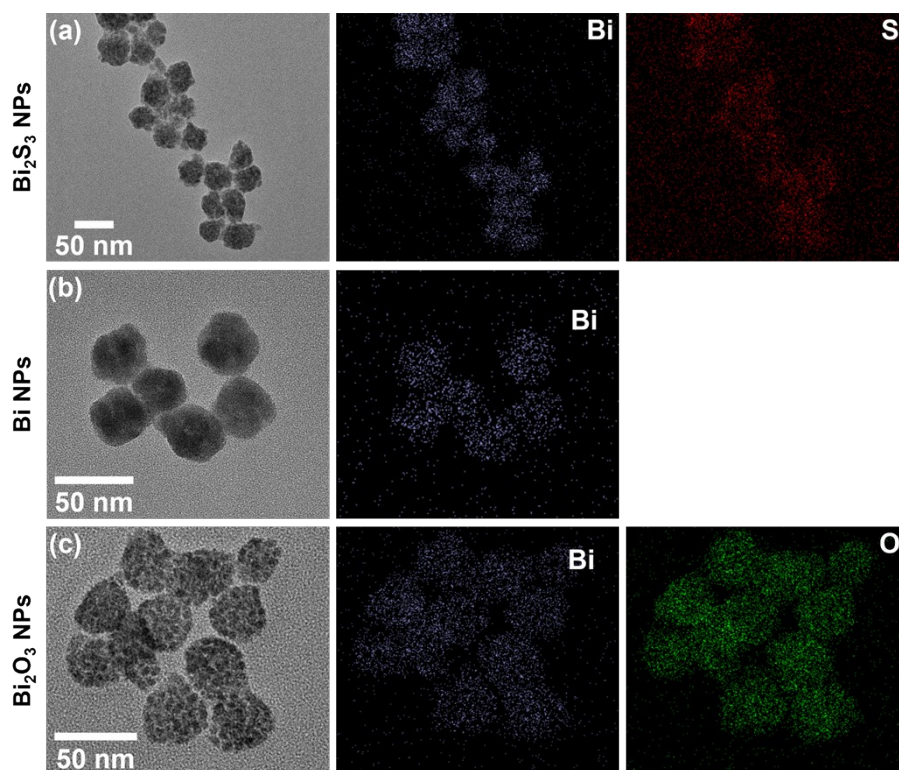


**Figure S2.** Elemental mapping images of the Bi<sub>2</sub>S<sub>3</sub> NPs (a), Bi NPs (b), and Bi<sub>2</sub>O<sub>3</sub> NPs (c), respectively.

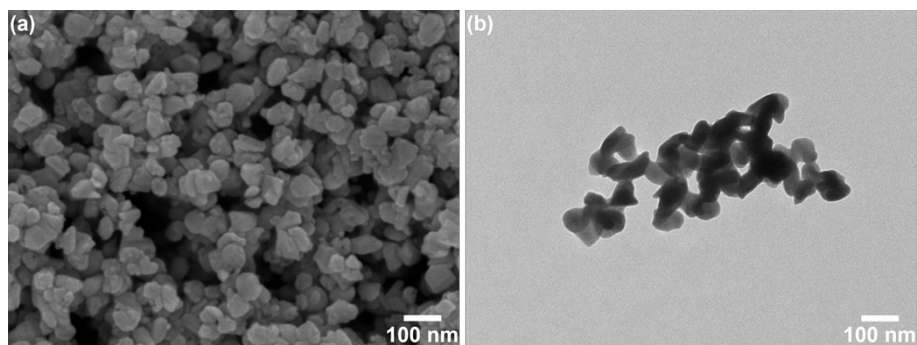


**Figure S3.** (a) SEM images and (b) TEM images of the  $\text{Bi}_2\text{S}_3$  NPs without PVP.

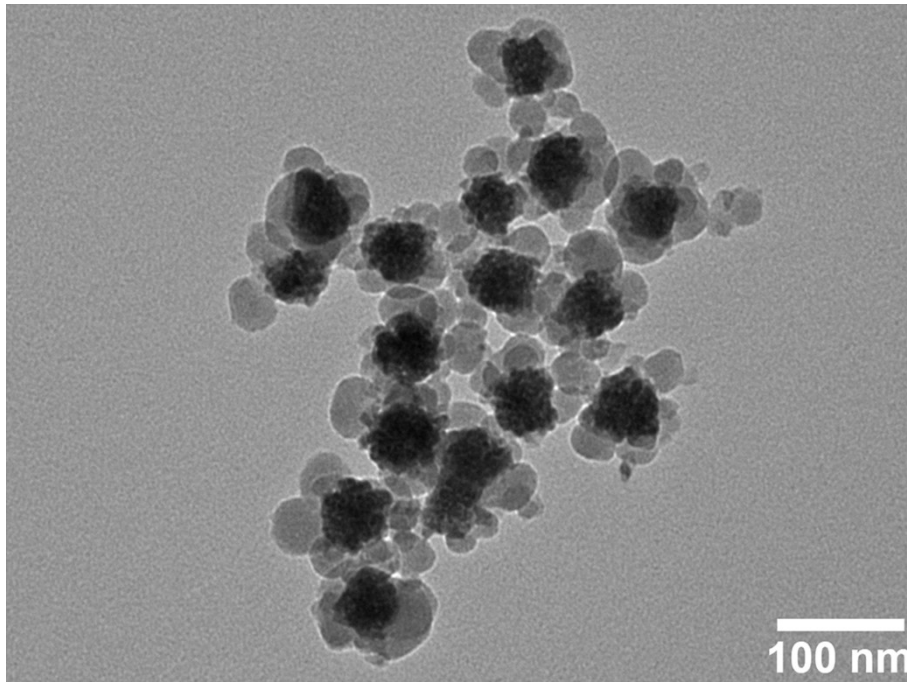


**Figure S4.** TEM images of the Bi<sub>2</sub>S<sub>3</sub>@SiO<sub>2</sub> NPs.

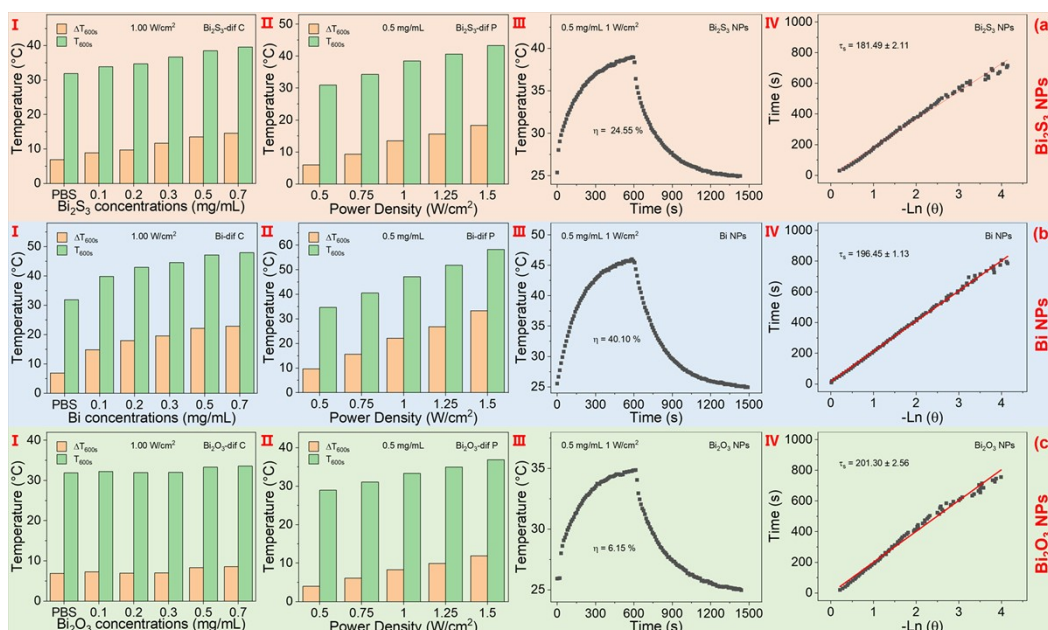


**Figure S5.** The temperatures after 600 s of irradiation by 808nm laser for solutions of Bi-based NPs at different concentrations (a-I, b-I, and c-I). The temperatures after 600 s of irradiation by 808nm laser at different working power densities for Bi-based NPs solution ( $0.5 \text{ mg mL}^{-1}$ ) are represented as (a-II, b-II, and c-II). The photothermal conversion efficiency of Bi-based NPs under 808 nm laser (a-III, b-III, and c-III). The plot of cooling time ( $t$ ) versus the negative natural logarithm of the temperature driving force ( $\theta$ ) obtained from the cooling stage (a-IV, b-IV, and c-IV).

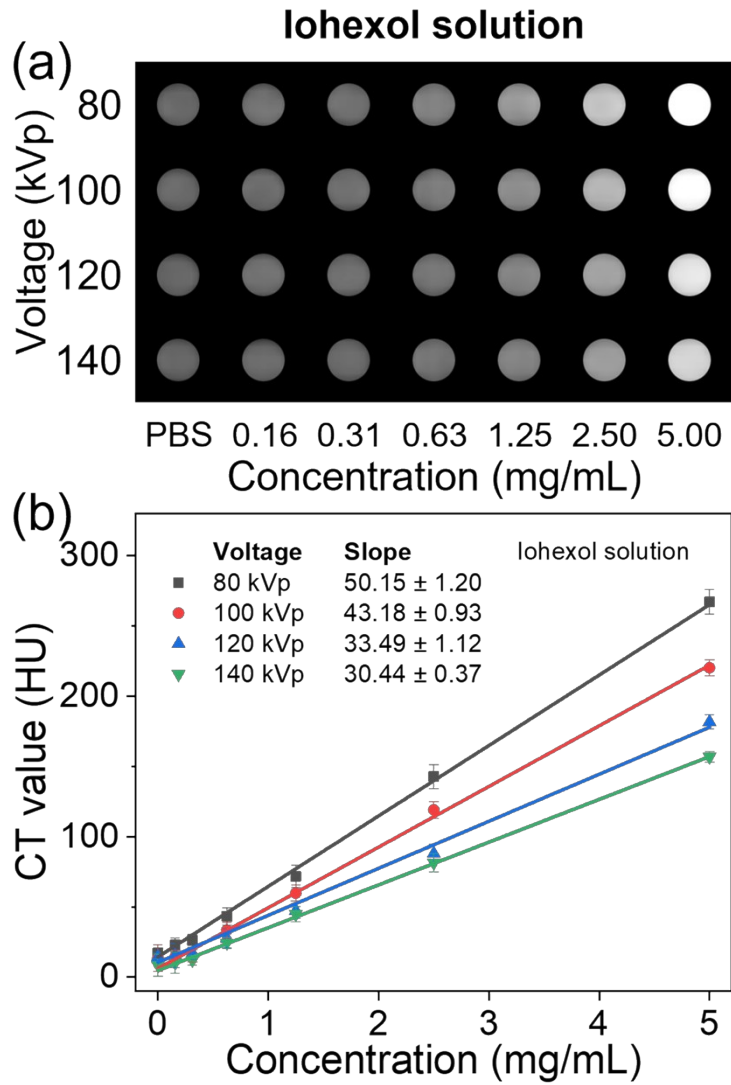


**Figure S6.** In vitro CT images of the commercial iohexol injection with different concentrations and work voltages.

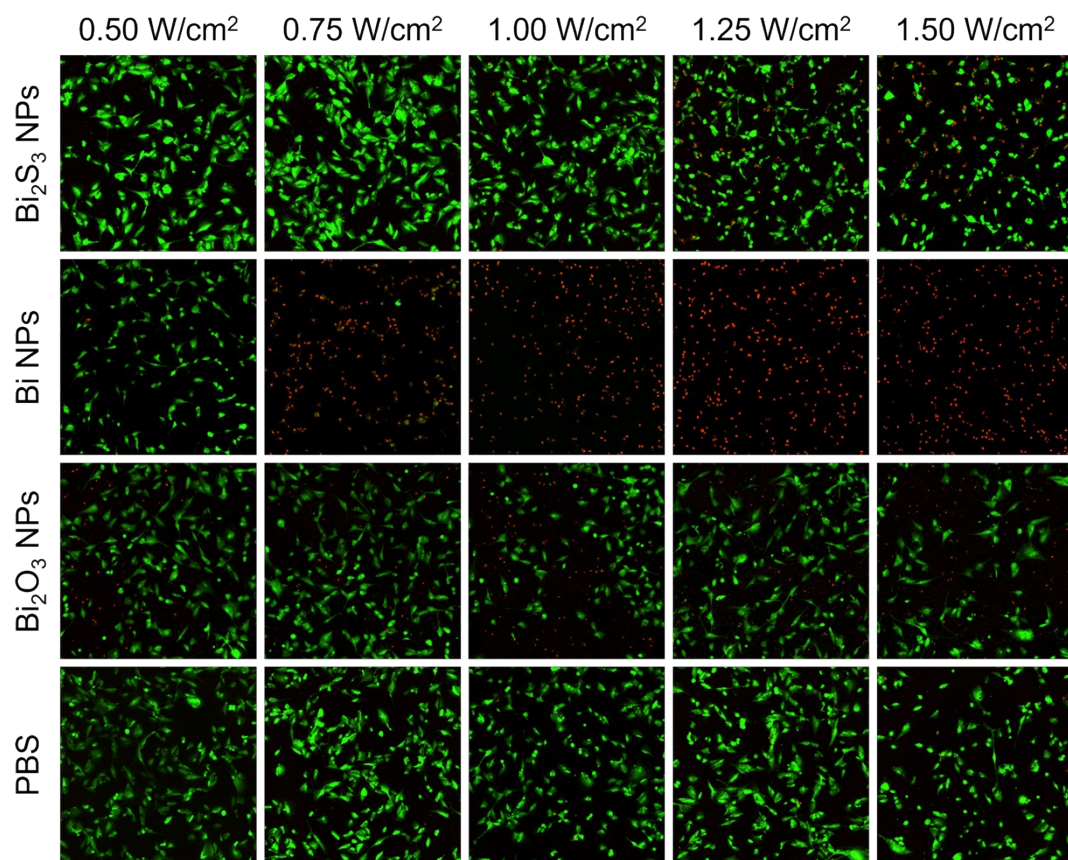


**Figure S7.** Fluorescence micrographs of Bi-based nanospheres at different power density NIR laser irradiation.

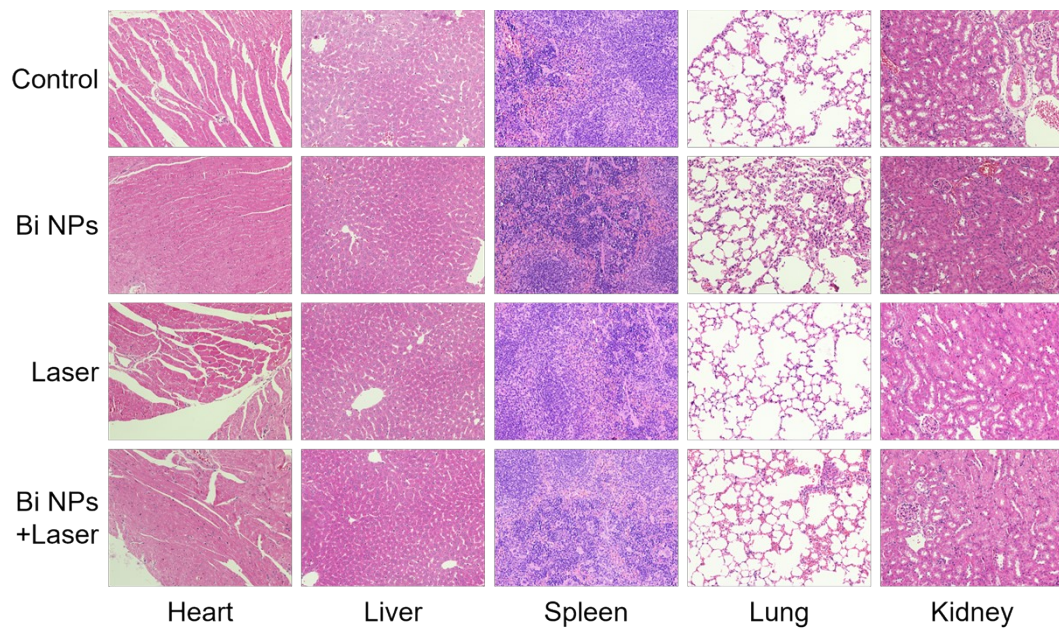


**Figure S8** H&E assay image of major organs from each group after 14 days of treatment.